Applied Soft Computing 113 (2021) 107986

Contents lists available at ScienceDirect

Applied Soft Computing

journal homepage: www.elsevier.com/locate/asoc

Frequency stabilization in interconnected power system using bat and harmony search algorithm with coordinated controllers

K. Peddakapu [a], M.R. Mohamed [a,*], P. Srinivasarao [b], P.K. Leung [c]

[a] College of Engineering, Universiti Malaysia Pahang, Kuantan, Malaysia
[b] Department of Electrical & Electronics Eng., Nalanda Institute of Eng. &Tech., A.P, India
[c] Faculty of Engineering & the Environment, University of Southampton, Highfield, United Kingdom

ARTICLE INFO

Article history:
Received 2 January 2021
Received in revised form 1 September 2021
Accepted 4 October 2021
Available online 19 October 2021

Keywords:
Automatic generation control
Hybrid BA–HSA
FACTS controllers
SMES
2DOF–TIDN
Interconnected system

ABSTRACT

Modern power system faces excessive frequency aberrations due to the intermittent renewable generations and persistently changing load demands. To avoid any possible blackout, an efficient and robust control strategy is obligatory to minimize deviations in the system frequency and tie-line. Hence, to achieve this target, a new two-degree of freedom-tilted integral derivative with filter (2DOF–TIDN) controller is proposed in this work for a two-area wind-hydro-diesel power system. To enhance the outcome of the proposed 2DOF–TIDN controller, its gain parameters are optimized with the use of a newly designed hybrid bat algorithm-harmony search algorithm (hybrid BA–HSA) technique. The effectiveness and superiority of hybrid BA–HSA tuned 2DOF–TIDN is validated over various existing optimization techniques like cuckoo search (CS), particle swarm optimization (PSO), HSA, BA and teaching learning-based optimization (TLBO). To further refine the system outcome in the dynamic conditions, several flexible AC transmission systems (FACTS) and superconducting magnetic energy storage (SMES) units are adopted for enriching the frequency and tie-line responses. The FACTS controllers like static synchronous series compensator (SSSC), thyristor-controlled phase shifter (TCPS), unified power flow controller (UPFC) and interline power flow controller (IPFC) are employed with SMES simultaneously. The simulation results disclose that the hybrid BA–HSA based 2DOF–TIDN shows superior dynamic performance with IPFC–SMES than other studied approaches. A sensitivity analysis is examined to verify the robustness of proposed controller under ±25% changes in loading and system parameters.

1. Introduction

An extensive power system involves numerous control areas, and every area of these control areas has different power generating units namely, gas, nuclear, and sustainable energy sources. The control areas are connected in one to one through alternating current (AC) or direct current (DC) lines and formed as an interconnected network. The interconnected multi-area power system contributes a good quality of power supply under steady and dynamic loading conditions. However, the interconnected system consistency, efficiency and the finest performance strongly depend on the system frequency. The desirable frequency of the system corresponds to the equalization of power production and the existed demand with considerable line losses.

The load demand on the power system is altering continuously and arbitrarily thereby, the fluctuations can occur in desirable system frequency. Hence, the interconnected power system may not be effective in operation or/and under control with diverse generating sources [1,2]. Over the past decades, there has been a dramatic increase in the number of interconnected power systems for alleviating the frequency variations with different control approaches. Automatic generation control (AGC) is one of the most productive approaches among various control methods. An automatic generation control (AGC) system is a power system which in addition to primary control incorporates secondary or supplementary controller. AGC system may be traditional or conventional where generating companies (GENCOs) generate as per the current load demand and in this way system frequency is controlled. Next, AGC system may be restructured or deregulated where GENCOs generate as per contracts made between GENCOs and distributing companies (DISCOs) duly approved by independent system operator (ISO). Deregulated system is an open system which creates competition among GENCOs and hence, cost of energy is likely to be reduced [3,4].

A large and fast-growing body of literature investigates several types of traditional control methods for AGC of multi-area systems [5,6]. The traditional controllers such as integral derivative

* Corresponding author.
E-mail address: rusllim@ump.edu.my (M.R. Mohamed).

https://doi.org/10.1016/j.asoc.2021.107986
1568-4946/

Nomenclature

AGC	Automatic Generation Control
GENCOs	Generation Companies
DISCOs	Distribution Companies
IO	Integer Order
2DOF	Two Degree of Freedom
TIDN	Tilted Integral Derivative Filter
PI	Proportional Integral
PID	Proportional Integral Derivative
ID	Integral Derivative
IDD	Integral Double Derivative
AC	Alternating Current
DC	Direct Current
FO	Fractional Order
FOPD	Fractional Order Proportional Derivative
FOI	Fractional Order Integral
PSO	Particle Swarm Optimization
BA	Bat Algorithm
HSA	Harmony Search Algorithm
TLBO	Teaching Learning-Based Optimization
WOA	Whale Optimization Algorithm
FACTS	Flexible AC Transmission System
SSSC	Static Synchronous Series Compensator
SMES	Superconducting Magnetic Energy Storage
STATCOM	Static Synchronous Compensator
ANFIS	Adaptive Neuro Fuzzy Inference System
HMCR	Harmony Memory Consideration Rate
ISE	Integral of Square Error
ITSE	Integral Time Square Error
IAE	Integral of Absolute Error
ITAE	Integral Time Absolute Error
ST	Settling Time
US	Undershoot
OS	Overshoot
HM	Harmony Memory
PAR	Pitch Adjusting Rate
BW	Bandwidth
JA	Jaya Algorithm
CS	Cuckoo Search
GWO	Grey Wolf Optimization
FA	Firefly Algorithm
PS	Pattern Search
RFBs	Redox Flow Batteries
TCPS	Thyristor-Controlled Phase Shifter
UPFC	Unified Power Flow Controller
IPFC	Interline Power Flow Controller

(ID), integral double derivative (IDD), proportional-integral (PI), proportional integral derivative (PID) are utilized to diminish the disparity in frequency and tie-line power at uncertainties [7,8]. Nevertheless, the conventional controllers do not yield the greater enhancement when abruptly changes in load demand and various kinds of nonlinearities exist in the system [9]. Since the conventional methods have distinct limitations, alternative control approaches are indispensable to be analysed for AGC of the interconnected system.

In recent years, the effect of interconnected multi-area system has been examined extensively using two degree of freedom (2DOF) and fractional order (FO) controllers [10,11]. R.K. Sahu et al. [12] have presented the 2DOF PID for mitigating the differences in system frequency with two thermal plants. Authors in [13,14] have applied the FO-based fuzzy PID controller in AGC of the hydrothermal interconnected system for enriching the system performance. Besides, few researchers [15,16] have concentrated on the combination of conventional controllers and connected in cascade form. Dash et al. [17] have cascaded the proportional-integral (PI) and proportional derivative (PD) with unequal power generating sources for alleviating the AGC obstacles. Saha and Saikia [18] have cascaded the PID with filter (PIDN) and FO-based PD called PIDN-FOPD for enriching the system stability. Although 2DOF and FO type control approaches are being estimated individually in the AGC of a multi-area interconnected system, the combined operation of both controllers is not yet to be studied. Consequently, it is substantial to be carried out the AGC system with dissimilar power-producing sources in an interconnected system.

To find the ideal gain values of various controllers and increase the system productivity, several optimization schemes are introduced in the AGC system. Diverse optimization approaches like grey wolf optimization (GWO) was developed to tune conventional controllers [19], simplified PSO-based PID [20], TLBO tuned PI/PID/2DOF PID [21], improved stochastic fractal search algorithm(ISFS)-based PID [22], Jaya algorithm (JA) optimized PIDN [23], whale optimization algorithm (WOA) tuned the combination of 2DOF-PIDN and FO based integral (I) called (2DOF PIDFOI) [24] methods are suggested in the AGC system for enriching system dynamic outcomes. Even though there were numerous investigations about AGC with several metaheuristic optimization approaches, limited of them were dedicated to hybrid algorithms. Therefore, it is crucial to conduct intensive research on the AGC problems with suggested controllers in the presence of hybrid algorithm.

Conversely, numerous studies [25,26] have been attempted to explain the performance of FACTS and energy management devices in the AGC of the interconnected system. Bhatt et al. [27] have presented the combination of TCPS and SMES for enhancing the frequency response in restructured (open market) power system. Another remarkable FACTS controller is interline power flow controller (IPFC), which can be employed with the redox flow batteries (RFBs) for diminishing the variations in tie-line power [28]. Sharma et al. [29] designed the adaptive neuro-fuzzy inference system (ANFIS)-based two-area system for boosting the system dynamic enactment with the assistance of the UPFC device. Although these investigations reported many interesting results, few works have examined with the coordination of energy storage devices and FACTS. In particular, the effect of AGC of the interconnected system with the combination of IPFC and SMES is yet to be explored.

In the light of above discussion, the main contribution of this work is clearly mentioned below:

1. The two-area AGC system has been designed with dissimilar power generating sources namely, wind, diesel and hydro.
2. The proposed 2DOF– TIDN controller is utilized as secondary controller and evaluated their effectiveness with other controllers, such as PID/2DOF PI/2DOF PID.
3. BA and HSA optimization methods are hybridized in this work for obtaining the requisite gain values and compared their performance with PSO, TLBO, CS, BA and HSA.
4. In order to enrich the system dynamic performance, the combination of SMES and FACTS controllers, such as TCPS/SSSC/UPFC/IPFC are employed simultaneously with hybrid BA–HSA-based 2DOF–TIDN.

5. The robustness of the suggested controller is carried out with ± 25% changes in all parameters of the two-area system and loading conditions.

The rest of this paper is organized as follows: Designing of two-area power system is discussed in Section 2. Section 3 describes the design of 2DOF–TIDN controller and selection of performance criterion. Section 4 explains the BA, HSA and hybrid BA–HSA methods. Modelling of IPFC and SMES are exhibited in Section 5. Performance analysis of hybrid BA–HSA algorithm is evaluated in Section 6. Results and discussion are demonstrated in Section 7. Sensitivity analysis of the system is represented in Section 8. Real time implementation and convergence analysis is explained in Section 9. Finally, Section 10 indicates the conclusion remarks of the paper.

2. Two-area power system

In this work, AGC of two-area three dissimilar power sources of the interconnected system has been researched with the distinct control techniques. The proposed two-area (wind-hydro-diesel) system is demonstrated in Fig. 1 [30,31]. The power rating of each area has considered as 1200 MW and system nominal values are mentioned in Appendix. Moreover, the transfer function model of each power production unit is shown in Fig. 1. Different controllers like PID, 2DOF PI, 2DOF PID, and 2DOF–TIDN are utilized as secondary controllers in the system and operated separately. For attaining ideal gain values of the controllers, distinct optimization methods are proposed, such as PSO, TLBO, HSA, CS, BA and hybrid BA–HSA. The two-area multi-power source system has been designed using MATLAB/Simulink software for analysis and coding. To decrease the changes in tie-line power and strengthen the system stability, energy management devices including SMES and numerous FACTS devices like SSSC, TCPS, IPFC, UPFC are co-ordinatively integrated in to the two-area system.

Modelling of two-area power system with dissimilar sources is illustrated in the below:

Power system transfer function is demonstrated as [30,31]:

$$G_{PS}(s) = \frac{K_{PS}}{1 + s.T_{PS}} \tag{1}$$

For wind system [30,31],

Model of the wind turbine is:

$$G_{WT}(s) = \frac{1}{1 + s.T_{p_2}} \tag{2}$$

Drive train model of wind is:

$$G_{DT}(s) = \left[\frac{K_P(1 + s.T_{P1})}{1 + s} . \frac{K_{P2}}{1 + s}\right] \tag{3}$$

For hydro system [30,31],

Mechanical model of the hydraulic governor is:

$$G_{HG}(s) = \left[\frac{K_1}{1 + s.T_{t_1}}\right]\left[\frac{1 + s.T_{R_1}}{1 + s.T_3}\right] \tag{4}$$

Hydro turbine model is:

$$G_{HT}(s) = \left[\frac{1 - s.T_{w_1}}{1 + 0.5\, s.T_{w_1}}\right] \tag{5}$$

For diesel system [30,31],

Diesel governor model is:

$$G_{DG}(s) = \frac{1}{1 + s.T_{gd}} \tag{6}$$

Diesel generator model is:

$$G_{DGen}(s) = \frac{1}{1 + s.T_{td}} \tag{7}$$

3. Design of 2DOF– TIDN using hybrid BA-HSA

Various industrial and engineering applications are served by conventional and integer-order (IO) control approaches for abating the nonlinear obstacles. The advantages of the traditional controllers are having the greatest structure, less cost, and productiveness for linear systems. Nonetheless, classical controllers are typically not suitable for high order and uncertainties endured systems. Recently, researchers have been shown increased interests to study the AGC system with fractional order (FO) type controllers. In this work, the properties of the two-degree freedom (2DOF) structure is amalgamated with tilt-integral–derivative-filter (TIDN) for abating the changes in frequency. The 2DOF controller has many closed-loop transfer functions and been employed independently. Moreover, it can be mitigated the difficulties of single degree freedom (IDOF) controllers for enriching the system stability under various loading conditions. The structure of the 2DOF controllers is represented in Fig. 2, having two inputs such as reference signal (R(s)) and measuring signal (Y(s)). On the other hand, TIDN controller is a sort of FO controllers. It has similar characteristics and dynamics as compared with proportional integral derivative filter (PIDN) controller [32]. Nevertheless, only the disparity is to be placed the tilted controller instead of proportional.

The schematic arrangement of the proposed 2DOF–TIDN controller is demonstrated in Fig. 3. The transfer function of TIDN controller is expressed as:

$$G_{TIDN}(s) = K_P\left(\frac{1}{S^{1/n}}\right) + K_i\left(\frac{1}{S}\right) + K_d\left(\frac{sN}{s + N}\right) \tag{8}$$

Similarly, C(s) and X(s) of the suggested 2DOF can be derived as [9,10]:

$$U(s) = \{bR(s) - Y(s)\}\frac{K_P}{S^{1/n}} + \{R(s) - Y(s)\}\frac{K_i}{S} + \{cR(s) - Y(s)\}\frac{K_d sN}{s + N} \tag{9}$$

Eq. (9) can be rewritten as:

$$U(s) = R(s)\left(b\frac{K_P}{S^{1/n}} + \frac{K_i}{S} + c\frac{K_d sN}{s + N}\right) - Y(s)\left(\frac{K_P}{S^{1/n}} + \frac{K_i}{S} + \frac{K_d sN}{s + N}\right) \tag{10}$$

From Eq. (10),

$$U(s) = \left(\frac{K_P}{S^{1/n}} + \frac{K_i}{S} + \frac{K_d sN}{s + N}\right) \times \left\{R(s)\left(\frac{b\frac{K_P}{S^{1/n}} + \frac{K_i}{S} + c\frac{K_d sN}{s+N}}{\frac{K_P}{S^{1/n}} + \frac{K_i}{S} + \frac{K_d sN}{s+N}}\right) - Y(s)\right\} \tag{11}$$

As per Fig. 2, it is observed that

$$U(s) = C(s)\{R(s).X(s) - Y(s)\} \tag{12}$$

The mathematical expressions of C(s) and X(s) can be determined through comparing the Eqs. (11) and (12):

$$C(s) = \frac{K_P}{S^{1/n}} + \frac{K_i}{S} + \frac{K_d sN}{s + N} \tag{13}$$

$$X(s) = \left(\frac{b\frac{K_P}{S^{1/n}} + \frac{K_i}{S} + c\frac{K_d sN}{s+N}}{\frac{K_P}{S^{1/n}} + \frac{K_i}{S} + \frac{K_d sN}{s+N}}\right) \tag{14}$$

3.1. Optimization constraints

The cascade combination of 2DOF and TIDN is worked as secondary controller in this AGC system for balancing the power

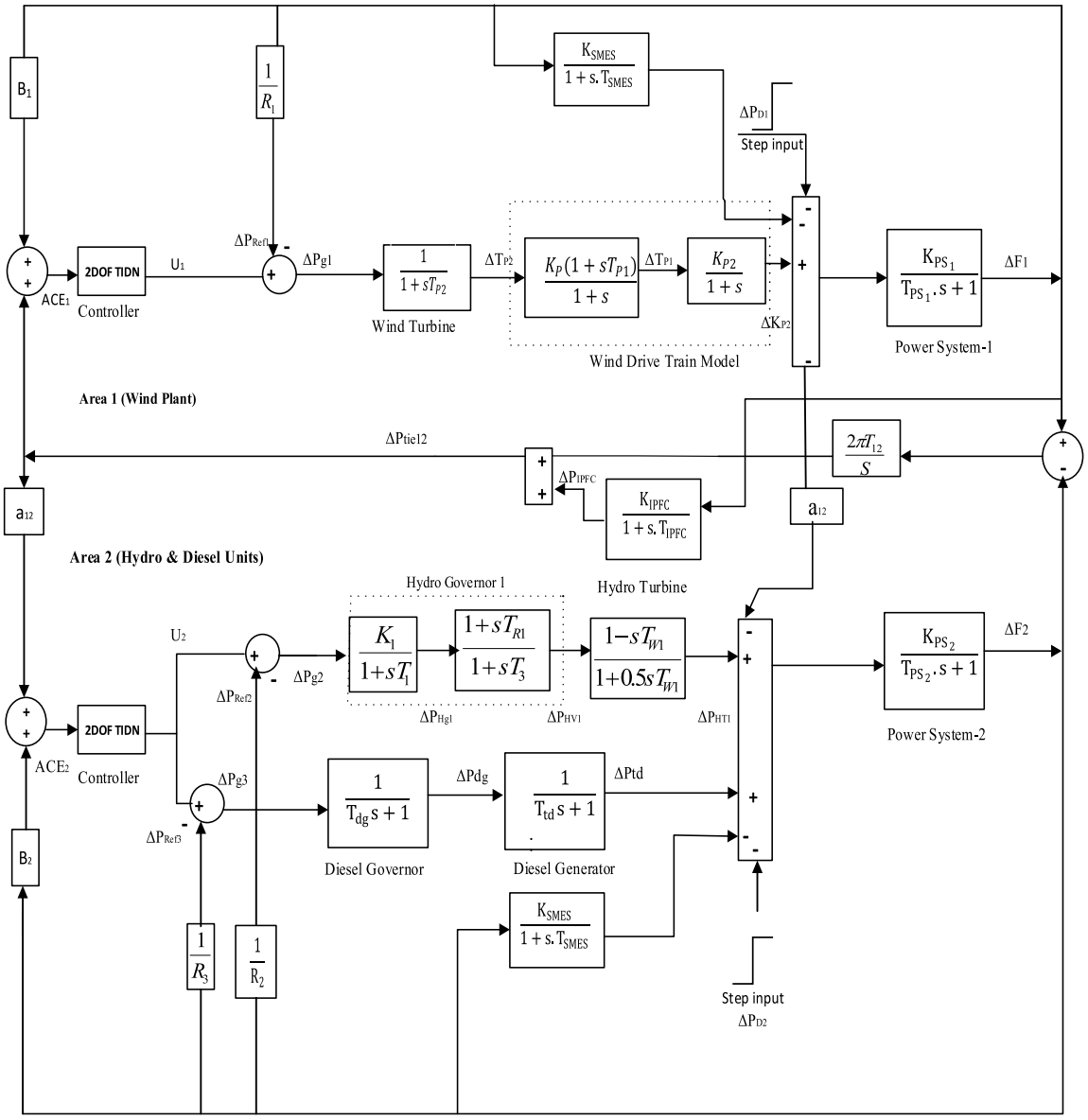

Fig. 1. Two-area (wind-hydro-diesel) power system.

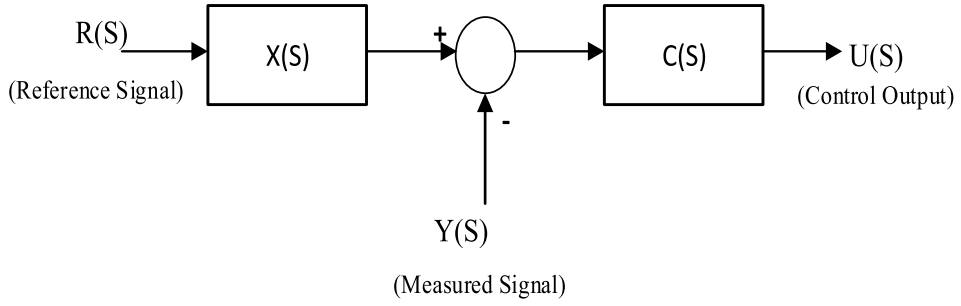

Fig. 2. The schematic representation of the 2DOF controller.

generation and demand with the integration of dissimilar power sources. However, an effective and robust optimization approach is required to obtain the suitable gain parameters of 2DOF–TIDN for controlling the variations in frequency. Hence, a new hybrid BA–HSA approach is proposed in this work for tuning the gains ($K_T/K_I/K_D/b/c/1/n/N$) of a 2DOF–TIDN controller. Various types of performance criterions are frequently considered in industry for designing the controllers. The performance criterions are integral of square error (ISE), integral time square error (ITSE), integral of absolute error (IAE), and integral time absolute error

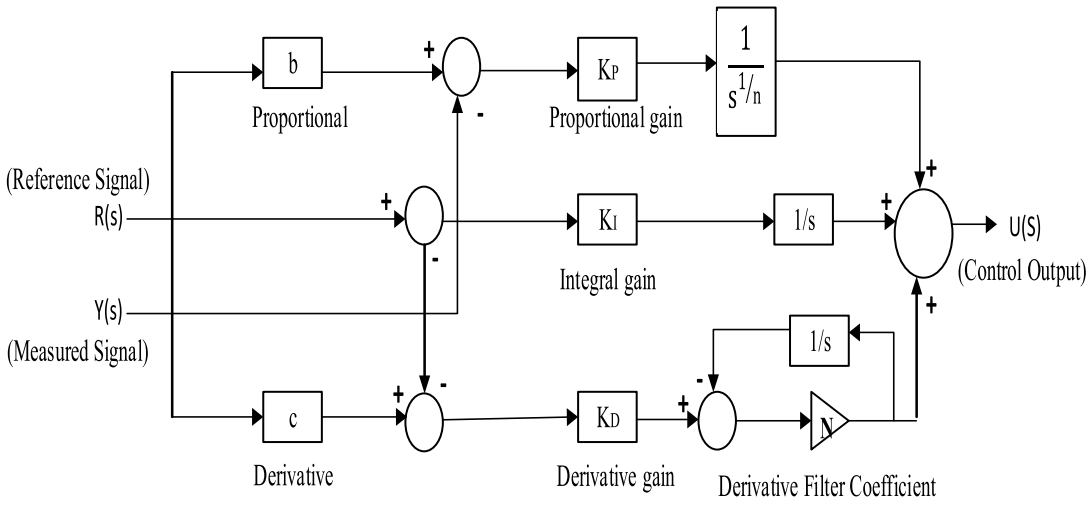

Fig. 3. The schematic arrangement of the 2DOF– TIDN controller.

(ITAE). The selection of performance criterion is the main aspect for the conceivable improvement in system performance. Due to their significant and effective performance, ITAE is considered as an objective function in this work and is demonstrated in Equ. (15).

$$J = ITAE = \int_0^{t_s} \{|\Delta F_1| + |\Delta F_2| + |\Delta P_{tie12}|\}\, t \cdot dt \tag{15}$$

Minimize J, subject to the following constraints of 2DOF–TIDN controller as:

$$K_{Pmin} < K_P < K_{Pmax}, K_{Imin} < K_I < K_{Imax}, K_{Dmin} < K_D < K_{Dmax},$$
$$b_{min} < b < b_{max},$$
$$N_{min} < N < N_{max}, c_{min} < c < c_{max}, {}^1/_{n_{min}} < {}^1/_n < {}^1/_{n_{max}} \tag{16}$$

The minimum (min.) and maximum (max.) values of the constraint parameters are considered between 0 and 1. The order of tilted (1/n) is used in between 0 and 2. The filter coefficient (N) is considered in between 0 and 100. For the purpose of a fractional order control, the frequency band $[\omega_l, \omega_h]$ is taken as [0.01, 50].

4. Optimization methods

4.1. BA technique

The bat algorithm (BA) approach is the most recent naturally inspired-based optimization algorithm, which was firstly proposed by X.S. Yang [33] in 2010. At initial population, each micro-bat in the BA utilizes a homologous pattern by executing echolocation process for upgrading its position.

Bat echolocation is a perceptual system in which bats provide loud ultrasonic pulses to the surrounding environment for hunting and navigation purposes. For bats, these transmitted pulses are turned into valuable information. Based on these emitted pulses, the bats can move and detect the obstacles and preys. In order to implement the structure of BA and idealize the echolocation attributes of bats, some assumptions are considered as:

1. Each bat uses the echolocation system; with this attribute they can detect food or surrounding object.
2. All bats fly in a random manner with velocity (V_i) at point X_i with a constant frequency (f_{min}), adjusting the loudness (A_0) and wavelength (λ) is to seek the food or find the nearest target. Additionally, bats can be altered the frequency/wavelength and rate of sound pulses automatically, in order to hit the target.
3. In nature, the loudness of the bats by emission can vary in different ways. However, in this algorithm assumed that the bats loudness can change from maximum (A_0) to minimum values (A_{min}).

Mathematical analysis

For every generation, the bats can move from population by upgrading its location and velocity. For these movements, the following expression is utilized as:

$$f_i = f_{min} + (f_{max} - f_{min})\,\beta \quad \text{where } \beta \epsilon\, [0, 1] \tag{17}$$
$$V_i{}^t = V_i{}^{t-1} + \left(x_i{}^t - x^*\right) f_i \tag{18}$$
$$x_i{}^t = x_i{}^{t-1} + V_i{}^t \tag{19}$$

where β is a random value and lies between 0 and 1. x^* is the current best solution among all bats. $V_i{}^t$ and $x_i{}^t$ indicate the velocity and the location of bats at every iteration t.

The new finest solution for every bat is generated by Eq. (20)

$$x_{new} = x_{old} + \partial A^t \tag{20}$$

where ∂ is a random value and remains between -1 and 1. The average loudness of each bat is represented as A^t with considerable step time (t).

The loudness of bats will be decreased when they detect the object or prey, and represents as below:

$$A_i{}^{t+1} = \propto .A^t \tag{21}$$

Similarly, the rate of sound pulses can be increased while the bats are identifying the target.

It can be expressed as:

$$r_i{}^{t+1} = r_i{}^0\,[1 - \exp(-\gamma t)] \tag{22}$$

where $\propto$ and γ are the constant numbers. In this study, these values are considered as $\propto = \gamma = 0.98$.

4.2. HSA technique

The HSA technique is one of the most significant optimization approaches for abating the optimization difficulties in distinct fields, this approach was suggested by Geem [34]. The HSA method depends on the musical accustoming used by musicians to obtain optimal harmony through a different possible grouping of musical pitches. The optimization operators of HSA are stated

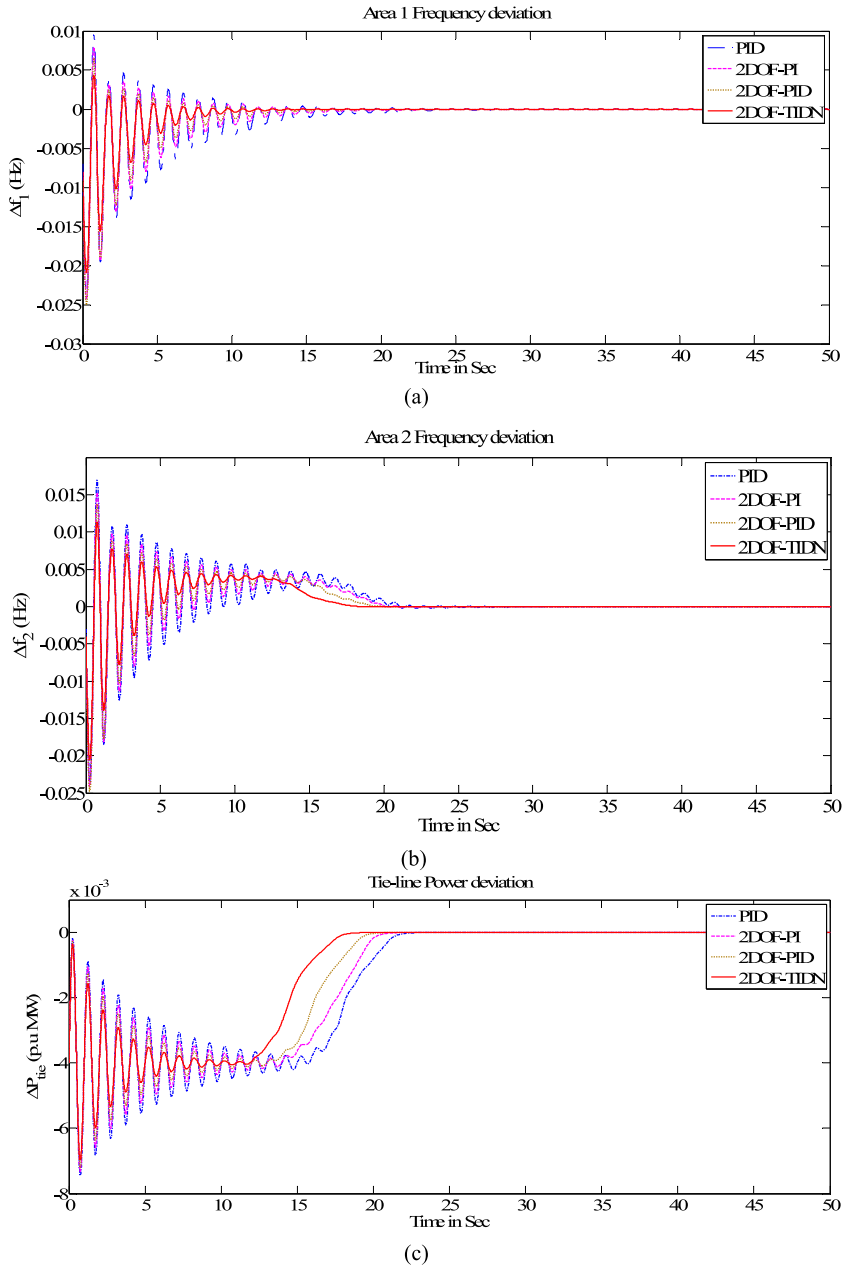

Fig. 4. Frequency and tie-line power deviations with suggested controllers.

as harmony memory (HM) and used for maintaining the resultant vectors and keeping in search space, as represented in (23).

$$HM = \begin{bmatrix} x_1^1 & x_2^1 & x_3^1 & \ldots\ldots & x_D^1 \\ x_1^2 & x_2^2 & x_3^2 & \ldots\ldots & x_D^2 \\ x_1^3 & x_2^3 & x_3^3 & \ldots\ldots & x_D^3 \\ .. & .. & .. & & .. \\ x_1^{HMS} & x_2^{HMS} & x_3^{HMS} & \ldots\ldots & x_D^{HMS} \end{bmatrix} \begin{bmatrix} fitness(x^1) \\ fitness(x^2) \\ fitness(x^3) \\ .. \\ fitness(x^{HMS}) \end{bmatrix} \quad (23)$$

In this matrix, HMS stands for harmony memory size. This matrix has numerous solution vectors that are stored in HM; other parameters of HS are pitch adjusting rate (PAR), harmony memory consideration rate (HMCR) and distance bandwidth (BW).

The detailed explanation of the HSA method can be discussed with the process of improvisation by a musician. For improvising, musicians have three possibilities, such as:

1. Play any famous piece of melody, which is matched to musician memory precisely as the HMCR.
2. Play melody equivalent to a famous piece in musician memory (so modifying the pitch considerably).
3. Completely play novel or random pitch from possible ranges.

The above three approaches are employed to be the optimized procedure. When each decision variable chooses one value in the HSA method, then it will be used anyone rule from above three rules for updating the HM. If the newly updated harmony vector in the HM is more suitable than the previously updated harmony vector, then a new harmony vector can be occupied the place of the previous harmony vector. Finally, this process is done repeatedly until getting a productive outcome. Three components are significant in HSA technique such as employment of HM, modifying the pitch and randomization. In a detailed discussion, the employment of HM is a very crucial process and

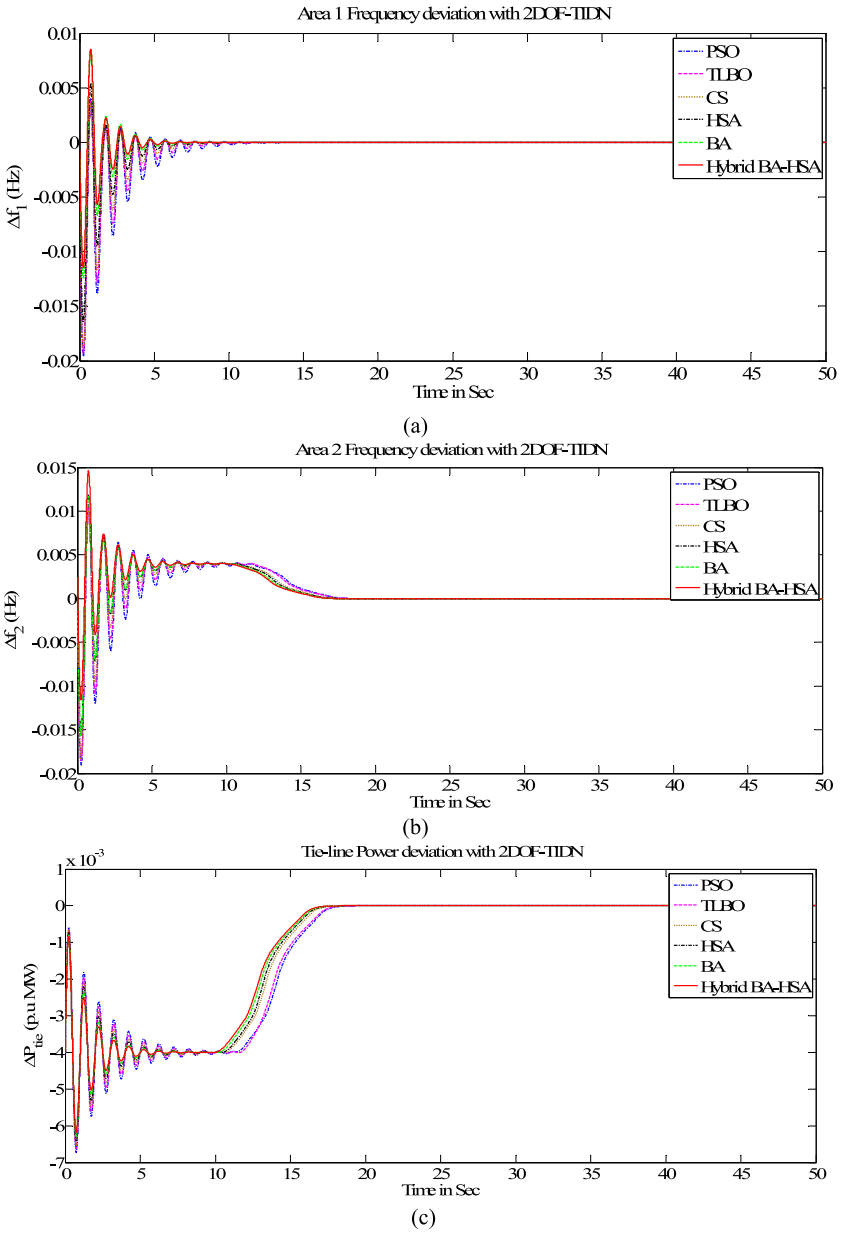

Fig. 5. Area 1 & area 2 frequency and tie-line power changes with optimized 2DOF–TIDN..

will be remained the finest harmonies in new harmony memory. To maintain this memory productively, the HMCR parameters should be kept within range (HMCR ϵ [0, 1]). If the HMCR is closed to 1, it indicates all harmonies are used in the HM. On the other hand, if the HMCR is very near to 0, it represents only a few finest harmonies are selected in the HM. Typically, the value of HMCR is 0.7∼0.95. To modify the pitch considerably in the second component, a suitable method is employed to modify the frequency effectively. If the previous pitch is x_{old}, then the new pitch (x_{new}) is produced by the following as:

$$x_{new} = x_{old} + BW\,(2\varepsilon - 1) \tag{24}$$

where BW and ε represent bandwidth and random number respectively. Also, BW is used to mitigate the local range of pitch modification.

The adjustment of pitch is equal to mutation operator in genetic algorithm. To reduce the degree of pitch adjustment, the parameters of the PAR shall be kept in the desirable range. If PAR closed to 1, then the outcome is varying continuously and the HSA may not be converged. If it is very near to 0, then the outcome has got minor change and the HSA method may be premature. Hence, the value of PAR in this simulation is 0.1 ∼0.5. In order to enhance the diversity of the outcomes of the HSA method, the randomization is required to look for a global optimum solution.

4.3. Hybrid BA-HSA

The general description of bat and harmony search algorithm (HSA) are explained separately in the previous sub-sections. In this study, BA and HSA methods are hybridized for acquiring the ideal gain values of the suggested controllers. The objective of hybrid BA/ HSA approach is to adjust the solutions with insignificant fitness, and enhance the search capability.

Typically, the BA approach is not to be performed the global search accurately as a result of they can easily trap into local optima. For example, at the initial iterations in BA, the exploitation (diversification) potentiality of the algorithm is high while exploration (intensification) is less. It is noted that, if new candidate

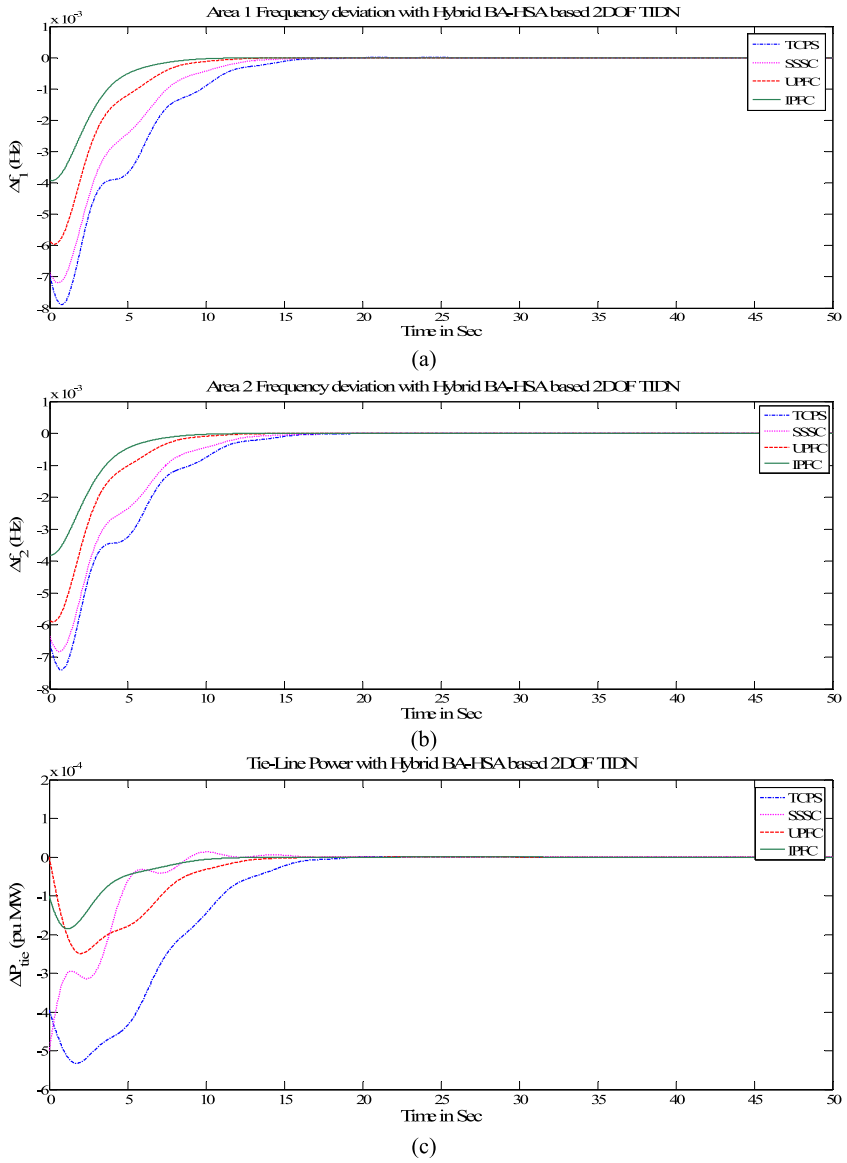

Fig. 6. Frequency and tie-line power changes with four FACTS controllers.

solutions are generated by using Eqs. (18) & (19) only, then the BA method gets good outcomes at exploration but it becomes not good at exploitation. If new candidate solutions are produced by Eq. (20) only, then the BA method demonstrates good outcomes at exploitation but it shows bad outcomes at exploration. Therefore, the algorithm can be easily trapped into the local optima. However, the balance between diversification (exploitation) and intensification (exploration) is very indispensable to the overall performance of optimization algorithm.

There are so many variants in BA and HSA approaches. However, the selection of this hybridization is to increase the BA convergence speed and escaping trapped into local optima by adding a pitch adjustment operation in HSA serving as mutation operator. Hence, this method can be made more feasible for realistic applications while protecting the standard characteristics of BA. Furthermore, the hybrid approach can investigate the latest search space with the help of mutation of the HSA, and BA is utilized to exploit the data of population for preventing trapping into local optima. The suggested mutation operator of hybrid HSA and BA has to be taken for two aspects. Firstly, insignificant solutions can acquire in many recent used attributes from effective solutions. Secondly, the exploration of the latest search space can be enhanced by mutation operator. Consequently, the exploration capabilities of HSA method and exploitation capabilities of BA can be amplified effectively.

For BA technique, since the search entirely depends on random walks, a rapid convergence cannot be assured. Depicted here for the first time, a key movement of adding mutation operator is made to the BA, including three minor enhancements. They can protect the original attributes of the BA method.

The first improvement is that it uses the constant frequency (f) and loudness (A) in place of variable f_i&$A_i{}^t$. Alike to BA, in BA–HSA, every bat in the population is indicated by its velocity ($V_i{}^t$), pulse rate ($r_i{}^t$), position ($x_i{}^t$), pre-ascertained frequency (f), loudness (A) in d-dimensional search space. The generation of new solutions can be expresses as:

$$V_i{}^t = V_i{}^{t-1} + \left(x_i{}^t - x^*\right) f \tag{25}$$

$$x_i{}^t = x_i{}^{t-1} + V_i{}^t \tag{26}$$

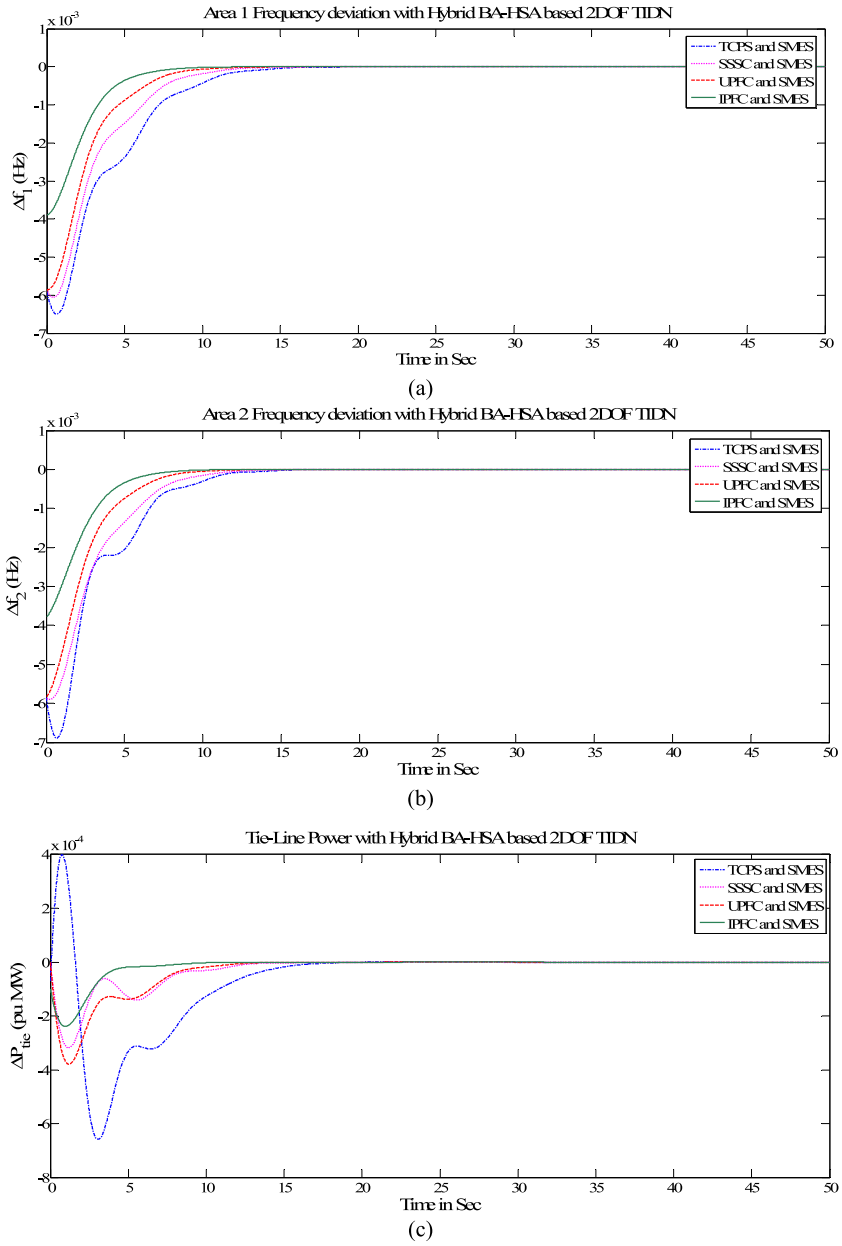

Fig. 7. Variations in frequency and tie-line with SMES and FACTS approaches.

where x^* represents the current best solution and it is located after identifying the best solution among all bats. In this study, f = 0.5 is considered.

The second enhancement is to merge the mutation operator in an endeavour to enrich the diversity of the population for increasing the search efficiency and convergence rate. For the local search section, once a solution is chosen among the current best solutions, each bat generates new solution by random walk (20). When ∂ is greater than pulse rate like $(\partial > r)$, where $\partial \epsilon [0, 1]$ is an arbitrary real value and drawn from a uniform distribution. When $\partial \leq r$, utilize the pitch adjustment operation in HSA and allocating as a mutation operator updating the HM vector with new solution to enrich the diversity of the population for enhancing the search efficiency.

The last enrichment is the incorporation of elitism scheme into the BA–HSA technique. To sustain the best solutions in the population, integrates some sort of the elitism in BA–HSA. It restrains the best solutions from being contaminated by pitch adjustment operator. It is worth to mention that incorporated elitism method to store the property of the bats that has the best solutions in BA–HSA process. Though pitch adjustment may corrupt its corresponding bat, it has stored and can return back to it if required.

The procedure of hybrid HSA and BA is explained clearly and mentioned in algorithm 1.

5. Modelling of IPFC and SMES

In recent years, several countries have concentrated on renewable/distributed/ sustainable energy sources for generating the extreme power than traditional units. Nonetheless, the challenging task in interconnected system is to be controlled the operation in an effective manner due to sudden changes in weather conditions. The tie-lines can be restricted in multi-areas with huge level of renewable/distributed/sustainable sources thus, may reduce the ability of tie-lines. Consequently, the interconnected multi-area system has to be improved by different advanced control approaches for renewable/sustainable power utilizations.

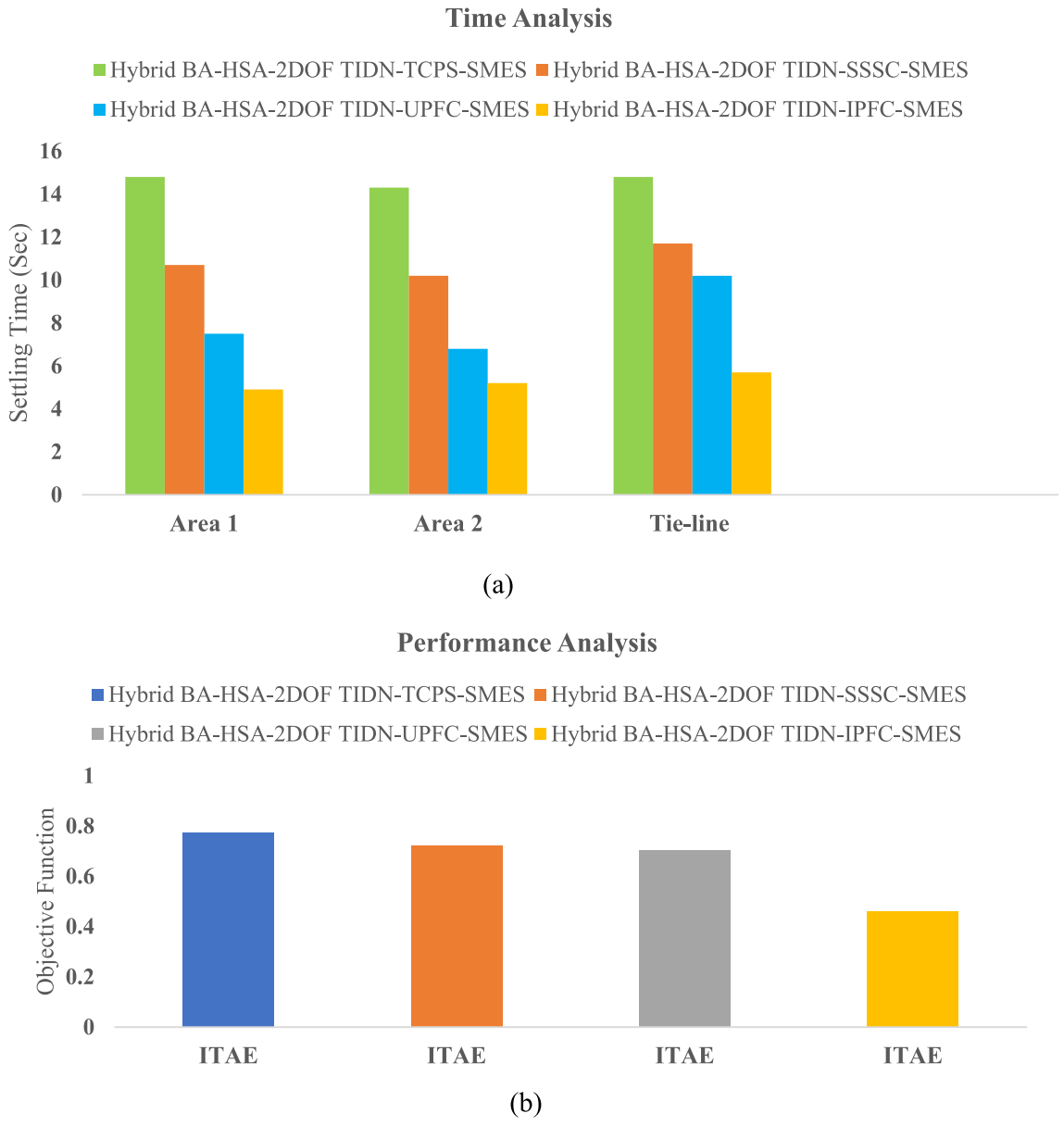

Fig. 8. Performance of the system with control methods.

Table 1
Unimodal functions.

Name	Formulation	Dimension	Range
Sphere	$F_1(x) = \sum_{i=1}^{D} x_i^2$	30	[−100, 100]
Rotated hyper-ellipsoid	$F_2(x) = \sum_{i=1}^{D} \left(\sum_{j=1}^{D} x_j \right)^2$	30	[−65, 65]
Rosenbrock	$F_3(x) = \sum_{i=1}^{D-1} \left[100 \left(x_{i+1} - x_i^2 \right)^2 + (x_i - 1)^2 \right]$	30	[−10, 10]

The joint coordinative operation of energy storage devices (ESDs) and FACTS controllers are needed for ameliorating the ability of tie-lines. In this work, a significant FACTS device called IPFC is utilized with the coordination of SMES for enriching the tie-line responses and sustaining the system dynamic stability.

The transfer functions model of the IPFC & SMES are represented as below [35]:

$$G_{IPFC}(s) = \frac{K_{IPFC}}{1 + s.T_{IPFC}} . \Delta F_i(s) \tag{27}$$

$$G_{SMES}(s) = \frac{K_{SMESi}}{1 + s.T_{SMESi}} . \Delta F_i(s) \tag{28}$$

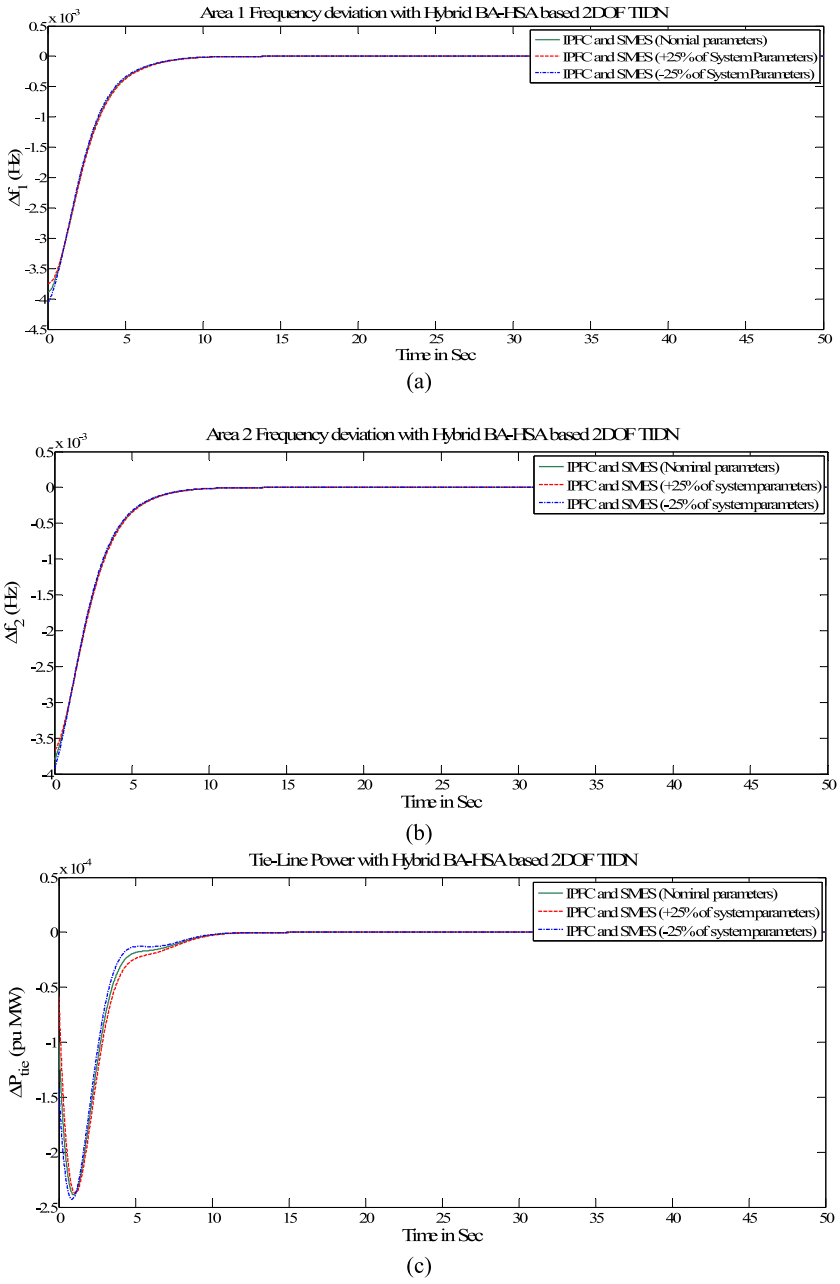

Fig. 9. Sensitivity analysis of the two-area system with proposed method.

Table 2
Multi-modal functions.

Name	Formulation	Dimension	Range
Rastrigin	$F_4(x) = \sum_{i=1}^{D} x_i^2 - 10\cos(2\Pi x_i) + 10$	30	[−5.12, 5.12]
Ackley	$F_5(x) = -20\exp\left(-0.2\sqrt{\frac{1}{n}\sum_{i=1}^{D} x_i^2}\right) - \exp\left(\frac{1}{n}\sum_{i=1}^{D}\cos(2\Pi x_i)\right)$+20+e	30	[−32, 32]
Griewank	$F_6(x) = \frac{1}{4000}\sum_{i=1}^{D} x_i^2 - \prod_{i=1}^{D}\cos\left(\frac{x_i}{\sqrt{i}}\right) + 1$	30	[−600, 600]

where, K_{SMESi}, K_{IPFC}, T_{SMESi}, T_{IPFC} are the gain and time constants of SMES & IPFC respectively. $\Delta F_i(S)$ is the deviation in frequency signal.

6. Performance analysis of hybrid BA-HSA algorithm

The effectiveness of hybrid BA–HSA algorithm is examined by using six benchmark test functions that are recorded in Tables 1 &

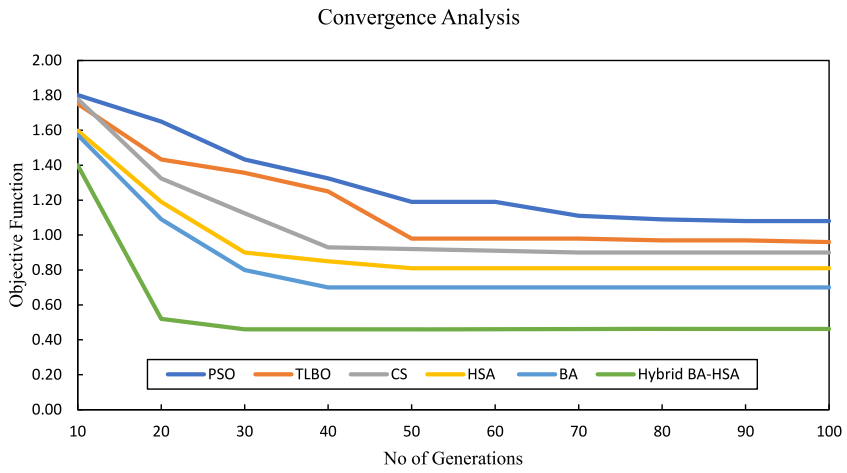

Fig. 10. Convergence analysis of applied algorithms.

Table 3
Statistical analysis for unimodal functions.

Function	Statistical measures	PSO	TLBO	CS	HSA	BA	Hybrid BA–HSA
F_1 (x)	Mean	2.782E+03	1.779E+03	4.527E+02	9.764E+03	4.917E+04	2.357E−01
	SD	1.124E+03	2.133E+03	9.618E+01	2.356E+03	1.989E+04	4.962E−01
F_2 (x)	Mean	1.682E+04	8.231E+03	2.248E+03	5.426E+04	2.702E+05	1.360E+01
	SD	7.556E+03	8.574E+03	5.653E+02	8.232E+03	1.357E+05	3.354E+01
F_3 (x)	Mean	8.279E+04	5.892E+03	1.193E+03	1.657E+05	4.916E+02	1.742E+02
	SD	6.561E+04	9.689E+03	3.987E+02	4.158E+04	6.275E+02	1.825E+02

Table 4
Statistical analysis for multi-modal functions.

Function	Statistical measures	PSO	TLBO	CS	HSA	BA	Hybrid BA–HSA
F_4 (x)	Mean	2.798E+02	5.842E+01	1.476E+02	1.690E+02	3.288E+02	1.125E+02
	SD	3.646E+01	1.927E+01	1.386E+01	1.595E+01	3.743E+01	4.031E+01
F_5 (x)	Mean	1.576E+01	5.938E+00	1.329E+01	1.652E+01	1.986E+01	5.732E+00
	SD	1.337E+00	2.581E+00	1.954E+00	7.937E−01	7.182E−04	1.531E+00
F_6 (x)	Mean	7.591E+01	1.977E+01	4.768E+00	8.150E+01	5.835E+02	1.301E−01
	SD	2.816E+01	1.928E+01	9.957E−01	1.689E+01	7.785E+01	1.382E−01

2 [22]. These benchmark functions are utilized to verify the exploration and exploitation capabilities of hybrid BA–HSA algorithm. As per Table 1, the unimodal test functions are utilized to check the exploitation performance of hybrid BA–HSA method. Similarly, the multi-modal functions (represented in Table 2) are used to test the exploration performance of hybrid BA–HSA method. In this suggested technique, 30 runs have been considered for ascertaining the mean and standard deviation (SD) values. Moreover, the proposed hybrid BA–HSA performance is evaluated with other studied approaches like PSO/TLBO/CS/HSA/BA. The acquired values are mentioned in Tables 3 & 4. As per Tables 3 & 4, its clearly observed that the hybrid BA–HSA method is produced the finest values over PSO/TLBO/CS/HSA/BA methods. Moreover, the exploration and exploitation capability of hybrid BA–HSA is enhanced under diverse benchmark functions.

Subsequently, non-parametric tests are conducted for ascertaining the performance of hybrid BA–HSA method. In this work, Wilcoxon and multiple comparison tests are presented [36]. The Wilcoxon signed-test is adopted to ascertain the p-values for evaluating the five groups, such as hybrid BA–HSA vs PSO, hybrid BA–HSA vs TLBO, hybrid BA–HSA vs CS, hybrid BA–HSA vs HSA, hybrid BA–HSA vs BA. For null hypothesis, it is assumed that there is no substantially variance between the five algorithms. The alternative hypothesis considers a significant variance between the five algorithms. The ascertained p-values by Wilcoxon signed-test are recorded in Table 5, where all p-values of hybrid BA–HSA versus other considered algorithms are <0.05 (5% significance). This is a strong affirmation against the null hypothesis, which means there is a significant variance between the values of the hybrid BA–HSA and other studied algorithms.

In addition to multiple comparisons, Friedman, Aligned Friedman and Quade tests are utilized in this study for evaluating the performance of the algorithms. For every test, the lowest rank of the algorithm is considered as an effective method. Table 6 indicates the computed ranks through Friedman test. As per numerical outcomes, the hybrid BA–HSA algorithm is obtained the lowest rank (1.66) as compared to other algorithms. The last two rows of Table 6 represent the statistic (20.021) and *p*-value of Friedman test. The *p*-value of the test is computed using the F (5, 25) distribution is 0.00592, hence, the null hypothesis is declined at high level of significance.

Table 7 presents the rank of each algorithm is determined through Aligned Friedman test. As shown in Table 7, the hybrid BA–HSA algorithm is attained the lowest rank than other studied algorithms. Moreover, the statistic and p-values of the Aligned Friedman test are 10.67, 0.00125 respectively. The *p*-value of this test is less than 0.05, so, this is a strong affirmation against the null hypothesis at high level of significance. Table 8 represents the rank computed through Quade test for each algorithm. Based on the results, the CS and hybrid BA–HSA is acquired the lowest ranks as compared with other four algorithms. The statistic and p-values of this test are 7.02, 1.402E−07 respectively.

Algorithm 1: Pseudocode of the hybrid HSA and BA

Begin
Step 1: Initialize the parameters: population of bats (P), A, f, V, r, HMCR, PAR, BW
Step 2: Ascertain the fitness function of the P bats and determine the finest f.
Step 3: While Generation (Gen) < Max_Gen **Do**
Classify the finest and worst bats basing on the fitness function for each bat and store the finest bats as KEEPBAT.
For *i*=1: All bats (NP) **do**
$V_i^t = V_i^{t-1} + (x_i^t - x^*)f_i$
$x_i^t = x_i^{t-1} + V_i^t$
If (rand>r) **then**
$x_{new} = x_{old} + \partial A^t$
End if
For j= 1: all elements (E) **do** //Mutate
% memory consideration
If (rand<HMCR) **then**
$r_1 = [NP * rand]$
$x_v(j) = x_{r_1}(j)$ where $r_1 \in (1,2, \ldots HSA)$
% modified pitch adjustment
If (rand<PAR) **then**
$x_v(j) = x_v(j) + BW(2 * rand - 1)$
Endif
Else
% random selection
$x_v(j) = x_{min,j} + rand * (x_{max,j} - x_{min,j})$
Endif
End for
% upgrade the HM
For i=1: new harmonies memory size (NHMS) **do**
If $f(x_v(j)) < f(x_{worst})$ **then**
$x_{worst} = x_v(j)$
End if
End for
Report the finest memory x_{finest} in the HM
Gen=Gen+1
Step 4: End while
Step: Visualize the outcomes
End

Table 5
p-values at 0.05 significance level using Wilcoxon signed test.

Comparison	p-value
Hybrid BA–HSA vs. PSO	1.315E−04
Hybrid BA–HSA vs. TLBO	9.984E−03
Hybrid BA–HSA vs. CS	1.637E−04
Hybrid BA–HSA vs. HSA	6.857E−04
Hybrid BA–HSA vs. BA	3.421E−04

Table 6
Friedman ranks.

Function	PSO	TLBO	CS	HSA	BA	Hybrid BA–HSA
F_1 (x)	4	3	2	5	6	1
F_2 (x)	4	3	2	5	6	1
F_3 (x)	5	4	3	6	2	1
F_4 (x)	5	1	4	3	6	2
F_5 (x)	3	2	4	5	6	1
F_6 (x)	5	3	2	6	4	1
Sum	26	16	17	30	30	7
Avg. rank	**4.33**	**2.66**	**2.83**	**5**	**5**	**1.166**
Statistic				**20.021**		
p-value				**0.00592**		

However, Friedman, Aligned Friedman, and Quade tests are only appropriate to identify the substantial differences over the total multiple comparison. Therefore, many post-hoc procedures are utilized in this study to ascertain the difference between the algorithms. Hybrid BA–HSA is considered as control method in this test. Table 9 represents the unadjusted and adjusted p-values for Friedman, Aligned Friedman and Quade tests. The investigations of the Friedman test demonstrate the substantial differences between hybrid BA–HSA and other suggested algorithms (PSO, TLBO, CS, BA, HSA). For Aligned Friedman and Quade tests, the hybrid BA–HSA is substantially superior to PSO, HSA and BA.

Table 7
Aligned friedman ranks.

Function	PSO	TLBO	CS	HSA	BA	Hybrid BA–HSA
F_1 (x)	26	27	21	28	33	3
F_2 (x)	29	31	24	30	36	16
F_3 (x)	35	32	23	34	25	22
F_4 (x)	17	13	10	11	18	19
F_5 (x)	6	9	8	4	1	7
F_6 (x)	15	14	5	12	20	2
Sum of ranks	128	126	91	119	133	69
Avg. rank	**21.3**	**21**	**15.16**	**19.83**	**22.16**	**11.5**
Statistic				**10.67**		
p-value				**0.00125**		

7. Results and discussion

7.1. Implementation of hybrid BA-HSA

This work contemplates delivering more exhaustive research about the effects of AGC with several control approaches. Two-area — three unequal power sources of the interconnected system have been considered for the analysis at perturbations. To diminish the variations in the system parameters, different kinds of controllers namely, PID, 2DOF PI, 2DOF PID, and 2DOF–TIDN are used as secondary controllers. Moreover, six optimization methods like PSO, TLBO, HSA, CS, BA, and hybrid BA–HSA are utilized in this study for tuning the suggested 2 DOF controllers.

For enriching the system performance, the amalgamation of SMES and four FACTS controllers namely, TCPS, UPFC, SSSC, IPFC are incorporated to the proposed system with the proposed optimization method. The suggested system has been designed using MATLAB/Simulink software for simulation evaluation, and represented in Fig. 1 [30,31]. The tuning process is repeated 30 times and selected the finest values among the 30 runs, which are related to minimum values of ITAE and utilized as controller parameters for the AGC of two-area system.

The gains of the proposed controllers are as follows: with PID for two-areas are, $K_P = 0.5892$, $K_I = 0.9498$, $K_D = 0.9254$ in area 1 and $K_P = 0.3536$, $K_I = 0.9725$, $K_D = 0.6827$ for area 2. With 2DOF PI, for area 1 is $K_P = 0.4925$, $K_I = 0.8245$, b = 0.6058, c = 0.2631, N = 86.25 and area 2 is $K_P = 0.2758$, $K_I = 0.4825$, b = 0.2659, c = 0.3615, N = 91.24. with 2DOF PID, for area 1 is $K_P = 0.3418$, $K_I = 0.9251$, $K_D = 0.3729$, b = 0.7258, c = 0.2468, N = 57.23 and area 2 is $K_P = 0.0252$, $K_I = 0.2928$, $K_D = 0.5216$, b = 0.3967, c = 0.1928, N = 46.27. Finally, for area 1 with 2DOF–TIDN is $K_P = 0.5418$, $K_I = 0.9723$, $K_D = 0.9753$, b = 0.1476, c = 0.0857, N = 39.45, 1/n = 8.2641. Whereas, for area 2, $K_P = 0.8624$, $K_I = 0.6258$, $K_D = 0.6289$, b = 0.0958, c = 0.1025, N = 55.35, 1/n = 12.249.

Fig. 4(a)–(c) illustrates the mitigation of frequency and tie-line power deviations with only PID, 2DOF PI, 2DOF PID and 2DOF–TIDN controllers. From Fig. 4(a), the 2DOF–TIDN controller diminished the changes in frequency at about 13 s whereas, 25 s for PID, 21 s for 2DOF PI and 18 s for 2DOF PID. Similarly, Fig. 4(b) represents that the frequency deviations in area 2 are mitigated rapidly with 2DOF–TIDN (16 s) than PID (27 s), 2DOF PI (22 s) and 2DOF PID (19 s). For tie-line power in Fig. 4(c), 16 s for 2DOF–TIDN, 18 s for 2DOF PID, 22 s for 2DOF PI and 24 s for PID. Based on the numerical results, the 2DOF–TIDN controller effectively diminished the fluctuations in frequency and tie-line power as examined with other studied approaches. The settling time (ST), overshoot (OS) and undershoot (US) are recorded in Table 10.

Furthermore, six optimization methods such as PSO, TLBO, CS, HSA, BA and hybrid BA–HSA are applied to tune the 2DOF–TIDN controller for obtaining the finest parameters to strengthening the system dynamic performance. The parameters of the suggested algorithms are mentioned in Table 11. The performance of various optimizations tuned 2DOF–TIDN is demonstrated in Fig. 5(a) for abating the changes in area 1 frequency. It is found that the hybrid BA–HSA optimized 2DOF–TIDN has damped out the oscillatory response at about 6 s whereas, 8 s for BA, 9 s for HSA, 10.5 s for CS, 12.3 s for TLBO, and 14 s for PSO. It has been observed that the mitigation rate of hybrid BA–HSA-based

Table 9
Outcomes of post-hoc procedure for all algorithms (hybrid BA–HSA is the control method).

Procedure	i	Algorithm	p-value	Holland	Rom	Finner	Li
Friedman	1	PSO	2.38E−8	1.49E−7	1.47E−7	1.49E−7	3.15E−8
	2	TLBO	1.792E−1	1.792E−1	1.788E−7	1.788E−7	1.788E−7
	3	CS	8.39E−3	0.0354	0.0348	0.0124	0.0103
	4	BA	2.01E−7	1.02E−6	9.58E−7	6.01E−7	2.32E−7
	5	HSA	4.39E−7	1.64E−6	1.63E−6	8.28E−7	5.22E−7
Aligned Friedman	1	BA	0.000894	0.00526	0.00522	0.00583	0.0075
	2	HSA	0.00192	0.0104	0.0097	0.0063	0.0157
	3	PSO	0.00289	0.0172	0.0115	0.0068	0.0212
	4	CS	0.4353	0.8212	0.8724	0.5825	0.7991
	5	TLBO	0.8921	0.8837	0.8615	0.8693	0.8677
Quade	1	HSA	0.0024	0.0148	0.0146	0.0148	0.0014
	2	PSO	0.0039	0.0214	0.0195	0.0156	0.0069
	3	BA	0.0114	0.0473	0.0441	0.0223	0.0211
	4	CS	0.1191	0.2224	0.2362	0.1401	0.1844
	5	TLBO	0.4525	0.4425	0.4428	0.4228	0.4428

Table 10
The values of the OS, US and ST with suggested controllers.

Controllers	Response	OS	US	ST
PID	ΔF_1	0.01	−0.021	25
	ΔF_2	0.017	−0.024	27
	ΔP_{tie}	0	−0.0075-	24
2DOF PI	ΔF_1	0.0087	−0.019	21
	ΔF_2	0.016	−0.022	22
	ΔP_{tie}	0	−0.0071	22
2DOF PID	ΔF_1	0.0058	−0.025	18
	ΔF_2	0.012	−0.024	19
	ΔP_{tie}	0	−0.0068	18
2DOF–TIDN	ΔF_1	0.0046	−0.021	13
	ΔF_2	0.01	−0.02	16
	ΔP_{tie}	0	−0.0065	16

Table 8
Quade test using the ranks in parentheses.

Function	Sample Range	Rank (Qi)	PSO	TLBO	CS	HSA	BA	Hybrid BA–HSA
F_1 (x)	1.98899E+04	4	(−4)(3)	(4)(4)	(−8)(2)	(8)(5)	(12)(6)	(−12)(1)
F_2 (x)	1.3567E+05	6	(−6)(3)	(12)(5)	(−12)(2)	(6)(4)	(18)(6)	(−18)(1)
F_3 (x)	6.5428E+04	5	(15)(6)	(5)(4)	(−10)(2)	(10)(5)	(−5)(3)	(−15)(1)
F_4 (x)	26.45	2	(2)(4)	(−2)(3)	(−6)(1)	(−4)(2)	(4)(5)	(6)(6)
F_5 (x)	2.5803	1	(−1)(3)	(3)(6)	(2)(5)	(−2)(2)	(−3)(1)	(1)(4)
F_6 (x)	77.7118	3	(6)(5)	(3)(4)	(−6)(2)	(−3)(3)	(9)(6)	(−9)(1)
Avg. Rank		**3.5**	**4**	**4.33**	**2.33**	**3.5**	**4.5**	**2.33**
Statistic	**7.02**							
p-value	**1.402E−07**							

Table 11
Proposed optimizations parameters.

Optimization	Parameters	Quantity
PSO	Population size	100
	PSO Parameter (C1)	1.5
	PSO Parameter (C2)	1.5
	PSO Inertia	0.73
	Number of iterations	90
TLBO	Population size	70
	Number of iterations	80
	Number of nests	50
CS	Discovery rate of alien eggs/solutions	0.25
	Number of iterations	70
	Harmony memory size (HMS)	40
	Harmony memory consideration rate (HMCR)	0.95
	Maximum pitch adjusting rate (PAR_{max})	2
HSA	PAR_{min}	2
	Maximum distance bandwidth (bw_{max})	0.9
	bw_{min}	0.4
	Number of iterations	50
	Population size	35
BA	Loudness	0.5
	Pulse rate	0.6
	Number of iterations	40
	Pulse rate	0.1
	Loudness	0.4
BA-HSA	HMCR	0.5
	PAR	0.1
	Number of iterations	30

2 DOF-TIDN settling times are 25%, 33.3%, 42.9%, 51.2% and 57.1% as compared with the BA, HSA, CS, TLBO, PSO respectively. On the other hand, the alleviations of area 2 frequency deviations with optimized 2DOF–TIDN is represented in Fig. 5(b). The results reveal that the hybrid BA–HSA based 2DOF–TIDN (8 s) controller has abated the deviations in frequency as quickly over BA (12 s), HSA (15 s), CS (15.5 s), TLBO (16.2 s), PSO (17 s). Besides, the suppression rate of BA–HSA based 2DOF–TIDN settling times are 33.33%, 46.66%, 48.38%, 50.61% and 52.94% as investigated with BA, HSA, CS, TLBO, PSO respectively.

Similarly, the reduction of tie-line power deviations with optimized 2DOF–TIDN controller is illustrated in Fig. 5(c). It is found that the hybrid BA–HSA reduces the oscillations in tie-line power at about 5.5 s, 12 s for PSO, 11 s for TLBO, 10 s for CS, 9.5 s for HSA, and 6.8 s for BA. Moreover, the reduction rate of hybrid BA–HSA-based 2DOF–TIDN is 54.2%, 50.0%, 45.0%, 42.1%, 19.1% as compared with PSO, TLBO, CS, HSA, BA respectively. The results of the numerical simulation indicate that the hybrid BA–HSA optimized 2DOF–TIDN renders better enhancement for abating the fluctuations in tie-line power as compared with other studied approaches. The numerical data of 2DOF–TIDN with suggested optimization methods are indicated in Table 12.

Subsequently, four FACTS devices like TCPS, UPFC, SSSC and IPFC are presented into the system for minimizing the variations of tie-line and frequency in the presence of hybrid BA–HSA-based 2DOF–TIDN. The differences of frequencies in area 1, area 2 and tie-line power with hybrid BA–HSA-based 2DOF–TIDN are depicted in Fig. 6(a)–(c) respectively. From Fig. 6(a), 15.5 s for TCPS, 11.2 s for SSSC, 7.7 s for UPFC, and 5.2 s for IPFC. For area 2 from Fig. 6(b), 14.8 s for TCPS, 11.9 s for SSSC, 8.5 s for UPFC and 5.6 s for IPFC. From Fig. 6(c), the tie-line power with FACTS controllers are, 15.4 s for TCPS, 12.2 s for SSSC, 10.3 s for UPFC and 5.2 s for IPFC. Based on the simulation results, the hybrid BA–HSA-based 2DOF–TIDN with IPFC illustrates the prominent performance than other FACTS approach for amplifying the system dynamic performance. The values of ST, ITAE, OS, and US are mentioned in Table 13. It is obvious from Table 13 that hybrid BA–HSA tuned 2DOF–TIDN with IPFC contributes a lower value of objective function (ITAE = 0.474) over TCPS (ITAE = 0.924), SSSC (ITAE = 0.840), UPFC (ITAE = 0.696).

Moreover, an energy storage device such as SMES is introduced into the system for working coordinative with presented FACTS controllers to improve the dynamic stability. Fig. 7(a)–(c)

Table 13
Values of the ST, ITAE, OS and US with FACTS controllers.

hybrid BA–HSA-2DOF–TIDN	Profile	OS	US	ST	ITAE
Without FACTS	ΔF_1	0.009	−0.011	6	1.325
	ΔF_2	0.015	−0.011	8	
	ΔP_{tie}	0	−0.0058	5.5	
TCPS	ΔF_1	0	−0.0079	15.5	
	ΔF_2	0	−0.0073	14.8	0.924
	ΔP_{tie}	0	−0.00052	15.4	
SSSC	ΔF_1	0	−0.0071	11.2	
	ΔF_2	0	−0.0069	11.9	0.840
	ΔP_{tie}	0	−0.00047	12.2	
UPFC	ΔF_1	0	−0.0059	7.7	
	ΔF_2	0	−0.0057	8.5	0.696
	ΔP_{tie}	0	−0.00024	10.3	
IPFC	ΔF_1	0	−0.004	5.2	
	ΔF_2	0	−0.0039	5.6	0.474
	ΔP_{tie}	0	−0.00018	8.8	

Table 14
ITAE, ST, OS and US performance with SMES and FACTS approaches.

Method	Profile	OS	US	ST	ITAE
Hybrid BA–HSA-2DOF–TIDN–TCPS–SMES	ΔF_1	0	−0.0062	14.8	
	ΔF_2	0	−0.0067	14.3	0.774
	ΔP_{tie}	0	−0.00063	14.8	
Hybrid BA–HSA-2DOF–TIDN–SSSC–SMES	ΔF_1	0	−0.0060	10.7	
	ΔF_2	0	−0.0059	10.2	0.723
	ΔP_{tie}	0	−0.00030	11.7	
Hybrid BA–HSA-2DOF–TIDN–UPFC–SMES	ΔF_1	0	−0.0059	7.5	
	ΔF_2	0	−0.0058	6.8	0.702
	ΔP_{tie}	0	−0.0003	10.1	
Hybrid BA–HSA-2DOF–TIDN–IPFC–SMES	ΔF_1	0	−0.0039	4.9	
	ΔF_2	0	−0.0038	5.2	0.462
	ΔP_{tie}	0	−0.00021	5.7	

Table 12
Performance assessment of 2DOF–TIDN with six optimization methods.

Method	Response	Parameter	PSO	TLBO	CS	HSA	BA	BA–HSA
2DOF–TIDN	ΔF_1	OS	0.0054	0.0047	0.0051	0.0042	0.008	0.009
		US	−0.019	−0.017	−0.015	−0.016	−0.013	−0.011
		ST	14	12.3	11.5	9	8	6
	ΔF_2	OS	0.013	0.012	0.011	0.013	0.014	0.015
		US	−0.018	−0.017	−0.016	−0.015	−0.014	−0.011
		ST	17	16.2	15.5	15	12	8
	ΔP_{tie}	OS	0	0	0	0	0	0
		US	−0.0068	−0.0065	−0.0063	−0.0061	−0.0060	−0.0058
		ST	12	11	10	9.5	6.8	5.5

Table 15
Hybrid BA–HSA tuned 2DOF–TIDN gain values with IPFC–SMES.

Compensator		2DOF–TIDN gains	Hybrid BA–HSA
IPFC–SMES	Area 1	K_P	1.5421
		K_I	1.9854
		K_D	1.9625
		N	38.452
		1/n	5.2641
		b	0.1476
		c	0.0857
	Area 2	K_P	1.8365
		K_I	1.6258
		K_D	0.6289
		N	59.294
		1/n	8.249
		b	0.0958
		c	0.1025

Table 16
Effectiveness of the proposed approach is compared with existed studies.

Approach	Settling time (ST)			ITAE
	ΔF_1	ΔF_2	ΔP_{tie}	
GA-based TCSC–SMES [26]	42.48	44.27	43.28	12.36
MFO-based TCSC–SMES [26]	26.06	27.29	37.19	3.64
TLBO optimized PIDD [21]	6.8	3.9	6.5	0.679
Proposed method	4.9	5.2	5.7	0.462

exhibits the deviations of frequencies in area 1, area 2 and tie-line power respectively. It is clearly indicated from Fig. 7(a), the hybrid BA–HSA-based 2DOF–TIDN with IPFC–SMES obtained less settling time (4.9 s) to settle down the oscillations in frequency response as compared to the UPFC–SMES (7.5 s), SSSC–SMES (10.7 s), TCPS–SMES (14.8 s). For area 2 in Fig. 7(b), 5.2 s for IPFC–SMES, 6.8 s for UPFC–SMES, 10.2 s for SSSC–SMES, 14.3 s for TCPS–SMES. Similarly, for tie-line power in Fig. 7(c), 5.7 s for IPFC–SMES, 10.1 s for UPFC–SMES, 11.7 s for SSSC–SMES and 14.8 s for TCPS–SMES. Moreover, the hybrid BA–HSA tuned 2DOF–TIDN with the combination of SMES and IPFC yields the lowest value of objective function (ITAE = 0.462) than UPFC–SMES (ITAE = 0.702), SSSC–SMES (ITAE = 0.723) and TCPS–SMES (ITAE = 0.774). The values of ITAE, ST, OS and US are presented in Table 14. It is apparently recognized from Fig. 7(a)–(c) and Table 14, the hybrid BA–HSA tuned the 2 DOF TIDN with SMES–IPFC are settled down the response variations in a small time and enhanced the dynamic stability. The gains of the 2DOF–TIDN with SMES–IPFC is presented in Table 15. The effectiveness of the proposed method is compared with the existed works and is shown in Table 16. Besides, performance of the system with control methods is demonstrated in Fig. 8.

8. Sensitivity analysis

A sensitivity analysis has been examined to check the robustness of the suggested hybrid BA–HSA tuned 2DOF–TIDN controller with the coordination of IPFC and SMES. To assess the robustness of the suggested controllers, all parameters (B_1, B_2, R_1, R_2, R_3, T_{12}) of the two-area system are altered from +25% to −25% in their nominal values (Appendix). Fig. 9(a)–(c) shows the frequency deviations of two-areas and their tie-line power respectively under normal and ±25% variations in the system parameters. From Fig. 9(a)–(c), it is apparently observed that the fluctuation rate of overshoot (OS) and undershoot (US) are changing in considerable range. Hence, the system will not be affected by ±25% variations in system parameters. The values of settling time (ST) with suggested methods are mentioned in Table 17.

Table 17
Values of settling time under sensitivity analysis.

Condition	%Change	Settling time (ST)		
		ΔF_1	ΔF_2	ΔP_{tie}
Nominal	0	13.23	12.52	13.64
Change in parameters	+25	13.43	12.64	13.95
(B_1, B_2, R_1, R_2, R_3, T_{12})	−25	13.52	13.72	14.21

As per Table 16, the values of ST for ΔF_1, ΔF_2, ΔP_{tie} are 13.23 s, 12.52 s, 13.64 s for nominal, 13.43 s, 12.64 s, 13.95 s for +25% variation in parameters, 13.52 s, 13.72 s, 14.27 s for -25% variations in parameters. The combination of IPFC and SMES with optimized 2DOF–TIDN has taken about to 15 s for stabilizing the variations in frequency under ±25% changes in system parameters (B_1, B_2, R_1, R_2, R_3, T_{12}). The similar approach has been observed in [26]. It is found that the suggested hybrid BA–HSA based 2D0F–TIDN renders finer dynamic performance with the collaboration of SMES and IPFC over studied approaches. It should be noted that the optimized gains of the controller at normal condition are not required to be reset for ±25% variation in the system parameters and loading conditions. Nevertheless, the proposed controller may not be assured to show the ideal gain values for ±50% changes in loading and system parameters (B_1, B_2, R_1, R_2, R_3, T_{12}).

9. Real-time implementation

As suggested, the proportion of control engineering has been reduced in R_2. It is worth to highlight that the controllers can be developed in offline during planning phase and then put into operation for online control of AGC system. Therefore, before the controllers are kept into action, the gains of the controllers are ascertained and they sustained constantly. Hence, the complexity of suggested hybrid BA–HSA technique to determine the gain values of 2DOF–TIDN will not escalate the computational burdens for online applications.

Additionally, the convergence rate of suggested algorithms is illustrated in Fig. 10. From the data in Fig. 10, it is apparent that hybrid BA–HSA ensures the finer optimal solution rapidly over PSO, TLBO, CS, HAS, BA before it moved the maximum iterations. Hence, the proposed hybrid BA–HSA method is most powerful technique with FACTS & other controllers for solving the obstacles in AGC of interconnected two-area system.

10. Conclusion

In this work, AGC of two-area three dissimilar sources (wind-hydro-diesel) of the interconnected system is considered for examinations. Moreover, the cascade combination of 2DOF and TIDN called 2DOF–TIDN is employed as a secondary controller for abating the deviations in system desirable frequency. Various optimization methods such as PSO, TLBO, CS, HSA, BA, and a new hybrid BA–HSA are presented to secure the requisite gain parameters of a new 2DOF–TIDN controller. It is found that the hybrid tuned 2DOF–TIDN yields finer performance with respect to mitigating the ST, US, OS and ITAE as compared with other studied approaches. Moreover, diverse FACTS controllers such as SSSC, TCPS, UPFC, IPFC are amalgamated into the two-area system with SMES for stabilizing the fluctuations in tie-line power and increasing the dynamic behaviour of the system. The findings reveal that the hybrid BA–HSA optimized 2DOF–TIDN with IPFC–SMES shows superior performance over other introduced FACTS controllers for improving the dynamic stability of the system. The robustness of the hybrid BA–HSA tuned 2DOF–TIDN is verified with ±25% variation in the system parameters in the presence of IPFC and SMES. It has been identified that the suggested method is robust at the nominal condition and not required to be reset for ±25% variation in the system parameters.

CRediT authorship contribution statement

K. Peddakapu: Acquisition of data, Writing – original draft, Analysis and/or interpretation of data, Writing – review & editing. **M.R. Mohamed:** Conception and design of study, Analysis and/or interpretation of data, Writing – original draft, Writing – review & editing. **P. Srinivasarao:** Writing – original draft, Writing – review & editing. **P.K. Leung:** Analysis and/or interpretation of data, Writing – review & editing.

Declaration of competing interest

The authors declare that they have no known competing financial interests or personal relationships that could have appeared to influence the work reported in this paper.

Acknowledgement

This project is supported by the Universiti Malaysia Pahang (UMP) through UMP's Doctoral Research Scheme (DRS) and UMP Postgraduate Research Grants Scheme (PGRS) - PGRS200322. All authors approved the version of the manuscript to be published.

Appendix

System data	F = 60 Hz, Power capacity of each area=1200 MW.
Power units' information	$K_{PS1} = K_{PS2} = 120\frac{Hz}{pu}$, $T_{PS1} = 6$, $T_{PS2} = 0.041$, $R_1 = R_2 = R_3 = 2.4\frac{Hz}{pu}$, $B_1 = B_2 = 0.425\ pu\frac{MW}{Hz}$, $T_{R1} = T_{R2} = 0.513s$, $T_1 = T_2 = T_3 = T_4 = 10\,s$, $K_1 = K_2 = 0.333$, $2\pi T_{12} = 0.545\ pu\frac{MW}{Hz}$, $a_{12} = a_{21} = -1$, $T_{W1} = T_{W2} = 1\,s$, $T_{dg} = 0.1\,s$, $T_{dt} = 8\,s$, $K_P = 1.25$, $K_{P2} = 1.4$.
FACTS and SMES details	$T_{TCPS} = 0.01\,s$, $T_{SSSC} = 0.31\,s$, $T_{UPFC} = 0.01\,s$, $T_{IPFC} = 0.01s$, $K_{TCPS} = 1$, $K_{SSSC} = 0.1802$, $K_{UPFC} = 0.01$, $K_{IPFC} = 0.12$, $T_{SMESi} = 0.03\,s$, $K_{SMESi} = 0.12$.

References

[1] D. Guha, P.K. Roy, S. Banerjee, Load frequency control of interconnected power system using grey wolf optimization, Swarm Evol. Comput. 27 (2016) 97–115.
[2] E. Rakhshani, P. Rodriguez, Inertia emulation in AC/DC interconnected power systems using derivative technique considering frequency measurement effects, IEEE Trans. Power Syst. 32 (5) (2016) 3338–3351.
[3] H. Haes Alhelou, M.E. Hamedani Golshan, M. Hajiakbari Fini, Wind driven optimization algorithm application to load frequency control in interconnected power systems considering GRC and GDB nonlinearities, Electr. Power Compon. Syst. 46 (11–12) (2018) 1223–1238.
[4] H.M. Hasanien, Whale optimisation algorithm for automatic generation control of interconnected modern power systems including renewable energy sources, IET Gener. Transm. Distrib. 12 (3) (2017) 607–614.
[5] M. Farahani, S. Ganjefar, Solving LFC problem in an interconnected power system using superconducting magnetic energy storage, Phys. C 487 (2013) 60–66.
[6] S. Padhy, S. Panda, A hybrid stochastic fractal search and pattern search technique based cascade PI-PD controller for automatic generation control of multi-source power systems in presence of plug in electric vehicles, CAAI Trans. Intell. Technol. 2 (1) (2017) 12–25.
[7] A. Khodabakhshian, R. Hooshmand, A new PID controller design for automatic generation control of hydro power systems, Int. J. Electr. Power Energy Syst. 32 (5) (2010) 375–382.
[8] R.K. Sahu, S. Panda, N.K. Yegireddy, A novel hybrid DEPS optimized fuzzy PI/PID controller for load frequency control of multi-area interconnected power systems, J. Process Control 24 (10) (2014).
[9] K.S. Simhadri, B. Mohanty, S.K. Panda, Comparative performance analysis of 2DOF state feedback controller for automatic generation control using whale optimization algorithm, Optim. Control Appl. Methods 40 (1) (2019) 24–42.
[10] T.K. Panigrahi, A. Behera, A.K. Sahoo, Novel approach to automatic generation control with various non-linearities using 2-degree-of-freedom PID controller, Energy Procedia 138 (2017) 464–469.
[11] V.H. Haji, C.A. Monje, Fractional order fuzzy-PID control of a combined cycle power plant using Particle Swarm Optimization algorithm with an improved dynamic parameters selection, Appl. Soft Comput. 58 (2017) 256–264.
[12] R.K. Sahu, S. Panda, U.K. Rout, D.K. Sahoo, Teaching learning based optimization algorithm for automatic generation control of power system using 2-DOF PID controller, Int. J. Electr. Power Energy Syst. 77 (2016) 287–301.
[13] Y. Arya, Improvement in automatic generation control of two-area electric power systems via a new fuzzy aided optimal PIDN-FOI controller, ISA Trans. 80 (2018) 475–490.
[14] Y. Arya, A new optimized fuzzy FOPI-FOPD controller for automatic generation control of electric power systems, J. Franklin Inst. 356 (11) (2019) 5611–5629.
[15] P. Dash, L.C. Saikia, N. Sinha, Automatic generation control of multi area thermal system using Bat algorithm optimized PD–PID cascade controller, Int. J. Electr. Power Energy Syst. 68 (2015) 364–372.
[16] M. Raju, L.C. Saikia, N. Sinha, Maiden application of two degree of freedom cascade controller for multi-area automatic generation control, Int. Trans. Electr. Energy Syst. 28 (9) (2018) e2586.
[17] P. Dash, L.C. Saikia, N. Sinha, Flower pollination algorithm optimized PI-PD cascade controller in automatic generation control of a multi-area power system, Int. J. Electr. Power Energy Syst. 82 (2016) 19–28.
[18] A. Saha, L.C. Saikia, Utilisation of ultra-capacitor in load frequency control under restructured STPP-thermal power systems using WOA optimised PIDN-FOPD controller, IET Gener. Transm. Distrib. 11 (13) (2017) 3318–3331.
[19] M.K. Debnath, R.K. Mallick, B.K. Sahu, Application of hybrid differential evolution–grey wolf optimization algorithm for automatic generation control of a multi-source interconnected power system using optimal fuzzy–PID controller, Electr. Power Compon. Syst. 45 (19) (2017) 2104–2117.
[20] S. Panda, B.K. Sahu, P.K. Mohanty, Design and performance analysis of PID controller for an automatic voltage regulator system using simplified particle swarm optimization, J. Franklin Inst. 349 (8) (2012) 2609–2625.
[21] R.K. Sahu, T.S. Gorripotu, S. Panda, Automatic generation control of multi-area power systems with diverse energy sources using teaching learning based optimization algorithm, Eng. Sci. Technol. Int. J. 19 (1) (2016) 113–134.
[22] Emre Çelik, Improved stochastic fractal search algorithm and modified cost function for automatic generation control of interconnected electric power systems, Eng. Appl. Artif. Intell. 88 (2020).
[23] S.P. Singh, T. Prakash, V.P. Singh, M.G. Babu, Analytic hierarchy process based automatic generation control of multi-area interconnected power system using Jaya algorithm, Eng. Appl. Artif. Intell. 60 (2017) 35–44.
[24] A. Saha, L.C. Saikia, Performance analysis of combination of ultra-capacitor and superconducting magnetic energy storage in a thermal-gas AGC system with utilization of whale optimization algorithm optimized cascade controller, J. Renew. Sustain. Energy 10 (1) (2018) 14103.
[25] S. Dhundhara, Y.P. Verma, Capacitive energy storage with optimized controller for frequency regulation in realistic multisource deregulated power system, Energy 147 (2018) 1108–1128.
[26] M. Nandi, C.K. Shiva, V. Mukherjee, Frequency stabilization of multi-area multi-source interconnected power system using TCSC and SMES mechanism, J. Energy Storage 14 (2017) 348–362.
[27] P. Bhatt, R. Roy, S.P. Ghoshal, Comparative performance evaluation of SMES–SMES, TCPS–SMES and SSSC–SMES controllers in automatic generation control for a two-area hydro–hydro system, Int. J. Electr. Power Energy Syst. 33 (10) (2011) 1585–1597.
[28] I.A. Chidambaram, B. Paramasivam, Control performance standards based load-frequency controller considering redox flow batteries coordinate with interline power flow controller, J. Power Sources 219 (2012) 292–304.
[29] G. Sharma, I. Nasiruddin, K.R. Niazi, R.C. Bansal, ANFIS based control design for AGC of a hydro-hydro power system with UPFC and hydrogen electrolyzer units, Electr. Power Compon. Syst. 46 (4) (2018) 406–417.
[30] K. Peddakapu, M.R. Mohamed, M.H. Sulaiman, P. Srinivasarao, A.S. Veerendra, P.K. Leung, Performance analysis of distributed power flow controller with ultra-capacitor for regulating the frequency deviations in restructured power system, J. Energy Storage 31 (2020) 101676.

[31] P.C. Sahu, R.C. Prusty, B.K. Sahoo, Modified sine cosine algorithm-based fuzzy-aided PID controller for automatic generation control of multi area power systems, Soft Comput. 24 (17) (2020).
[32] N.R. Babu, S.K. Bhagat, L.C. Saikia, T. Chiranjeevi, Application of hybrid crow-search with particle swarm optimization algorithm in AGC studies of multi-area systems, J. Discrete Math. Sci. Cryptogr. 23 (2) (2020) 429–439.
[33] S. Yılmaz, E.U. Küçüksille, A new modification approach on bat algorithm for solving optimization problems, Appl. Soft Comput. 28 (2015) 259–275.
[34] M. Gheisarnejad, An effective hybrid harmony search and cuckoo optimization algorithm based fuzzy PID controller for load frequency control, Appl. Soft Comput. 65 (2018) 121–138.
[35] J. Morsali, K. Zare, M.T. Hagh, A novel dynamic model and control approach for SSSC to contribute effectively in AGC of a deregulated power system, Int. J. Electr. Power Energy Syst. 95 (2018) 239–253.
[36] J. Derrac, S. García, D. Molina, F. Herrera, A practical tutorial on the use of nonparametric statistical tests as a methodology for comparing evolutionary and swarm intelligence algorithms, Swarm Evol. Comput. 1 (2011) 3–18.